

Long noncoding RNA SNHG20 promotes prostate cancer progression via upregulating DDX17

Xing-Cheng Wu, Wei-Gang Yan, Zhi-Gang Ji, Guo-Yang Zheng, Guang-Hua Liu

Department of Urology, Peking Union Medical College Hospital, Chinese Academy of Medical Sciences and Peking Union Medical College, Peking, China

Submitted: 25 December 2018; **Accepted:** 20 April 2019

Online publication: 6 June 2019

Arch Med Sci 2021; 17 (6): 1752–1765

DOI: <https://doi.org/10.5114/aoms.2019.85653>

Copyright © 2019 Termedia & Banach

Corresponding author:

Guang-Hua Liu
Department
of Urology
Peking Union Medical
College Hospital
Chinese Academy
of Medical Sciences
and Peking Union
Medical College
Peking, China
E-mail:
liuguanghuapumch@163.com

Abstract

Introduction: Accumulating evidence has revealed the critical roles of long noncoding RNAs (lncRNAs) in various cancers. LncRNA SNHG20 has been shown to be a cancer-associated lncRNA in several cancers with diverse mechanisms. However, the clinical references, biological roles, and mechanisms of action of SNHG20 in prostate cancer (PCa) are still unclear.

Material and methods: The expression of SNHG20 in PCa tissues and cell lines was detected by RT-qPCR. The correlations between SNHG20 expression and clinicopathological features were analyzed by χ^2 test. The roles of SNHG20 in PCa cell proliferation and migration were detected by CCK-8, EdU incorporation, and transwell assays. The regulatory mechanisms of SNHG20 on DDX17 were detected by dual luciferase reporter assay, RT-qPCR, and western blot.

Results: SNHG20 is highly expressed in PCa tissues and cell lines. High expression of SNHG20 is positively correlated with high Gleason score and advanced tumor stage. Functional experiments revealed that overexpression of SNHG20 promotes PCa cell proliferation and migration. SNHG20 knockdown represses PCa cell proliferation and migration. Mechanistically, SNHG20 was verified to act as a competing endogenous RNA (ceRNA) to upregulate DDX17. DDX17 is also highly expressed and has oncogenic roles in PCa. Furthermore, the expression of DDX17 is significantly positively correlated with that of SNHG20 in PCa tissues. Depletion of DDX17 reverses the oncogenic roles of SNHG20 in PCa.

Conclusions: These data showed that SNHG20 promotes PCa cell proliferation and migration via acting as a ceRNA to upregulate DDX17. This study also suggested that SNHG20 may be a potential novel therapeutic target for PCa.

Key words: prostate cancer, long noncoding RNA, competing endogenous RNA, DDX17, proliferation, migration.

Introduction

Prostate cancer (PCa) is the second most frequent cancer and the fifth leading cause of cancer-related death in men worldwide [1]. The estimated number of new PCa cases is 1,276,106 and the estimated number of deaths caused by PCa is 358,989 in 2018 worldwide [1]. With the development of the economy, the incidence of PCa is obviously increasing, particular in developing countries [2]. Due to the great advances of therapeutic strategies, including surgery, radiotherapy, molecular targeted therapy, and immunotherapy, the survival of most early PCa patients is relatively

good [3]. However, the efficiencies of therapies for PCa diagnosed at advanced stages with metastases or castration resistance are only palliative [4, 5]. Thus, further revealing the underlying molecular mechanisms and identifying novel therapeutic targets for aggressive PCa are urgent [6].

Increasing evidence has shown that most of the human transcriptome consists of non-coding RNAs, but not mRNAs [7]. Long noncoding RNAs (lncRNAs) are a class of regulatory non-coding RNAs with no protein coding potential and longer than 200 nucleotides in length [8, 9]. Relative to the 21,000 genes, more than 58,000 lncRNAs have been identified in humans [7]. Among these lncRNAs, many were further found to be deregulated in various diseases, including cancers [10–14]. Among these differently expressed lncRNAs, some were further verified to have important roles in a variety of pathophysiological statuses [15–21]. The lncRNAs were reported to regulate the various biological behaviors of cancer cells, including proliferation, cell cycle, apoptosis, senescence, migration, invasion, growth, metastasis, drug resistance, and so on [22–26].

The mechanisms of action of lncRNAs are complex and diverse. They could directly interact with proteins, mRNAs, microRNAs (miRNAs) and/or DNAs, and further change the locations, expressions and/or functions of their interacting partners [27–29]. Several lncRNAs were revealed to competitively sponge common miRNAs and relieve the suppressive roles of miRNAs on their targets [30–32]. Therefore, these lncRNAs upregulate the expression of targets of common miRNAs [33, 34]. These lncRNAs were classified as competing endogenous RNAs (ceRNAs) [35, 36].

lncRNA SNHG20 was reported to be highly expressed and predict poor prognosis in colorectal cancer, hepatocellular carcinoma, gastric cancer, osteosarcoma, cervical cancer, and non-small cell lung cancer [37–42]. SNHG20 was also revealed to generally play oncogenic roles in these cancers via different mechanisms. SNHG20 upregulates ZFX expression via sponging miR-495-3p in gastric cancer [39]. SNHG20 induced epithelial-mesenchymal transition-associated genes in osteosarcoma [40]. SNHG20 upregulates ADAM10 expression via sponging miR-140-5p in cervical cancer [41]. SNHG20 epigenetically silences p21 in non-small cell lung cancer [42]. These different mechanisms of action of SNHG20 in different cancers implied the disease-specific function manners of SNHG20 and the need to further investigate the expression, functions, and mechanisms of action of SNHG20 in other cancers.

Thus, we further explored the expression pattern, roles, and mechanisms of action of SNHG20 in PCa. Our data revealed that SNHG20 also func-

tions as an oncogene in PCa. Furthermore, we identified a novel mechanism of action of SNHG20 in PCa.

Material and methods

Clinical samples

The PCa tissues and adjacent noncancerous tissues were collected from 68 PCa patients who underwent tumor resection in Peking Union Medical College Hospital (Beijing, China) with written informed consent. All clinical samples were immediately frozen in liquid nitrogen for further use. The study was carried out in accordance with the Helsinki Declaration and was approved by the Ethics Committee of Peking Union Medical College Hospital.

Cell culture

The human PCa cell lines PC3 and DU145 and the normal prostate epithelial cell line RWPE-1 were acquired from the American Type Culture Collection (ATCC, Manassas, VA, USA). RWPE-1 cells were maintained in Keratinocyte Serum Free Medium (KSFM) kit (Invitrogen, Carlsbad, CA, USA). PC3 cells were maintained in F12K Medium (Invitrogen) supplemented with 10% fetal bovine serum (FBS) (Invitrogen). DU145 cells were maintained in Eagle's Minimum Essential Medium (Invitrogen) supplemented with 10% FBS (Invitrogen). The cells were incubated in a humidified atmosphere at 37°C with 5% CO₂.

Vectors construction

SNHG20 full-length sequences were PCR-amplified with the Thermo Scientific Phusion Flash High-Fidelity PCR Master Mix (Thermo Fisher Scientific, Inc., Rockford, IL, USA) and the primers 5'-CGGGATCCAAGTTGCTGACGGAGCTACTT-3' (sense) and 5'-GGAATTCGGAATCAAAGTGGTTATTCCA-3' (antisense). The PCR products were then inserted into the BamH I and EcoR I sites of pcDNA3.1(+) vector (Invitrogen), named as pcDNA-SNHG20. One pair of cDNA oligonucleotides specifically inhibiting SNHG20 were synthesized and inserted into the GenePharma supersilencing shRNA expression vector pGPU6/Neo (GenePharma, Shanghai, China). The target site is 5'-GCCTAGGATCATCCAGGTTTG-3'. The DDX17 overexpression vector was purchased from FulenGen (Guangzhou, China) (Catalog, EX-Z3245-M02). DDX17 specific shRNA expression vector was purchased from FulenGen (Guangzhou, China) (Catalog, HSH000626-nU6). The 3'UTR of DDX17 was PCR-amplified with the Thermo Scientific Phusion Flash High-Fidelity PCR Master Mix and the primers 5'-CGAGCTCCACTCAAGTGGTAGTGACT-3'

(sense) and 5'-GCTCTAGAGAAAACAAGATGATGG-TATC-3' (antisense). The PCR products were then inserted into the Sac I and Xba I sites of pmirGLO vector (Promega, Madison, WI, USA), named as pmirGLO-DDX17.

Stable cell lines construction

In order to construct SNHG20 stably overexpressed PCa cells, pcDNA-SNHG20 was transfected into PC3 and DU145 cells with Lipofectamine 3000 (Invitrogen) in accordance with the protocol. Forty-eight hours after transfection, PC3 and DU145 cells were treated and selected with neomycin for 4 weeks. In order to construct SNHG20 stably depleted PCa cells, SNHG20 specific shRNA was transfected into PC3 and DU145 cells with Lipofectamine 3000 (Invitrogen). Seventy-two hours after transfection, PC3 and DU145 cells were treated and selected with neomycin for 4 weeks. In order to construct DDX17 stably overexpressed PCa cells, the DDX17 overexpression vector was transfected into PC3 cells with Lipofectamine 3000 (Invitrogen). Forty-eight hours after transfection, PC3 cells were treated and selected with puromycin for 4 weeks. In order to construct SNHG20 stably overexpressed and concurrently DDX17 stably depleted PCa cells, DDX17 specific shRNA was transfected into SNHG20 stably overexpressed PC3 cells with Lipofectamine 3000 (Invitrogen). Seventy-two hours after transfection, PC3 cells were treated and selected with puromycin for 4 weeks.

RNA extraction and real-time quantitative polymerase chain reaction (RT-qPCR)

Total RNA was extracted from indicated tissues and cells with the TRIzol Regent (Invitrogen) in accordance with the protocol. The RNA quality and concentration were determined using NanoDrop ND-2000/2000C. Next, equal quantification of RNA was subjected to reverse transcription with the M-MLV Reverse Transcriptase (Promega) in accordance with the protocol. Subsequently, the cDNA was used as a template for real-time quantitative polymerase chain reaction (RT-qPCR) with SYBR Green Master Mix (Takara, Dalian, China) and gene specific primers. GAPDH served as an internal control. Primer sequences were as follows: for SNHG20, 5'-AGCAACCACTATTTCTTCC-3' (sense) and 5'-CCTTGGCGTGTATCTATTAT-3' (antisense); for DDX17, 5'-TACGCCGAAAGAAGGAGATT-3' (sense) and 5'-ACTAAGAGCCAACGGAAATC-3' (antisense); for GAPDH, 5'-TGACTTCAACAGCGACACCA-3' (sense) and 5'-CACCTGTTGCTGTAGCCAAA-3' (antisense). The quantification of RNA expression was normalized to GAPDH and calculated using the $2^{-\Delta\Delta Ct}$ method.

Western blot

Cell lysates were prepared from indicated PCa cells with the RIPA lysis buffer (Beyotime, Shanghai, China). Protein concentration was measured using BCA Protein Assay Kit (Beyotime) in accordance with the protocol. Subsequently, proteins were fractionated by 10% sodium dodecyl sulfate-polyacrylamide gel electrophoresis (SDS-PAGE) and electroblotted onto 0.45 μ m polyvinylidene fluoride (PVDF) membrane (Millipore, Boston, MA, USA). After being blocked in 5% non-fat milk for 2 h at room temperature, the membranes were incubated with primary antibodies against DDX17 (Abcam, Hong Kong, China) or GAPDH (Affinity, Changzhou, China) overnight at 4°C. After being washed three times, the membranes were incubated with a HRP-conjugated secondary antibody (Beyotime) and detected with an ECL-Plus kit (Amersham Biosciences, Piscataway, NJ, USA).

Cell proliferation assays

Cell proliferation was assessed using Cell Counting Kit-8 (CCK-8) and ethynyl deoxyuridine (EdU) incorporation assays. For CCK-8 assay, indicated PCa cells were plated at 2×10^3 cells/well into 96-well plates. After incubation for the indicated time, CCK-8 solution (Dojindo Laboratories, Kumamoto, Japan) was added into the wells. Optical density (OD) values at 450 nm at indicated time points were detected using an automatic enzyme-linked immune detector. EdU incorporation assay was carried out using the Cell-Light EdU Apollo 643 In Vitro Imaging Kit (RiboBio, Guangzhou, China) following the protocol. Results were detected with a Zeiss fluorescence photomicroscope (Carl Zeiss, Oberkochen, Germany) and counted based on five randomly chosen visual fields.

Transwell migration assay

Indicated PCa cells resuspended in serum-free medium were plated at 2×10^3 cells/well into 24-well transwell chambers (BD Biosciences, San Jose, CA, USA). Fresh medium containing 10% FBS was added into the lower portion of the chamber. After incubation for 48 h, the cells remaining in the upper chambers were removed. The cells that migrated to the lower surfaces of the wells were fixed with methanol and stained with 0.5% crystal violet. The number of migratory cells was detected using a Zeiss fluorescence photomicroscope and counted based on five randomly chosen visual fields.

Dual luciferase reporter assay

pmirGLO or pmirGLO-DDX17 was co-transfected with SNHG20 overexpression vector or

SNHG20 knockdown vector into PC3 cells using Lipofectamine 3000 (Invitrogen). After incubation for 48 h, the Firefly luciferase activity and Renilla luciferase activity were measured using the Dual-Luciferase Reporter Assay System (Promega) in accordance with the protocols.

Statistical analysis

GraphPad Prism 5.0 (La Jolla, CA, USA) was used to perform statistical analyses. For comparisons, Wilcoxon signed-rank test, Pearson χ^2 test, one-way ANOVA followed by Dunnett's multiple comparison tests, Student's *t*-test, and Pearson correlation analysis were carried out as indicated. $P < 0.05$ was considered as statistically significant for all analyses.

Results

Expression level of SNHG20 in human PCa tissues and cell lines

We first analyzed the expression level of SNHG20 in 68 pairs of PCa tissues and adjacent noncancerous tissues by RT-qPCR. The results showed that SNHG20 was markedly increased in PCa tissues compared with adjacent noncancerous tissues (Figure 1 A). Subsequently, we analyzed the relationship between SNHG20 expression level and clinicopathological characteristics in these 68 PCa cases. As shown in Table I, the increased level of SNHG20 was positively associated with high Gleason score and advanced tumor stage. Next, we measured the expression level of SNHG20 in PCa cell lines PC3 and DU145 and the human prostate epithelial cell line RWPE-1 by RT-qPCR. As shown in Figure 1 B, SNHG20 was also markedly increased in PCa cell lines compared with the prostate epithelial cell line.

Enhanced expression of SNHG20 promotes PCa cell proliferation and migration

In order to investigate the roles of SNHG20 in PCa, SNHG20 stably overexpressed and control PC3 and DU145 cells were constructed through the stable transfection of SNHG20 overexpression vector (pcDNA-SNHG20) or control empty vector (pcDNA3.1). The enhanced expression of SNHG20 was verified by RT-qPCR (Figures 2 A and B). CCK-8 assays indicated that enhanced expression of SNHG20 markedly promoted cell proliferation of PC3 and DU145 cells (Figures 2 C and D). Moreover, EdU incorporation assays further verified that enhanced expression of SNHG20 markedly promoted cell proliferation of PC3 and DU145 cells (Figures 2 E and F). Subsequently, we investigated the roles of SNHG20 in PCa cell migration. Transwell assays revealed that enhanced expression of

SNHG20 significantly promoted cell migration of PC3 and DU145 cells (Figures 2 G and H). These data suggested that enhanced expression of SNHG20 promotes PCa cell proliferation and migration.

Knockdown of SNHG20 represses PCa cell proliferation and migration

In order to completely explore the roles of SNHG20 in PCa, SNHG20 stably depleted and control PC3 and DU145 cells were constructed through the stable transfection of SNHG20 knockdown vector (sh-SNHG20) or negative control vector (sh-NC). The knockdown of SNHG20 was verified by RT-qPCR (Figures 3 A and B). CCK-8 assays indicated that knockdown of SNHG20 significantly repressed cell proliferation of PC3 and DU145 cells (Figures 3 C and D). EdU incorporation assays further verified that knockdown of SNHG20 markedly repressed cell proliferation of PC3 and DU145 cells (Figures 3 E and F). Subsequently, we investigated the roles of SNHG20 knockdown on PCa cell migration. Transwell assays revealed that knockdown of SNHG20 significantly repressed cell migration of PC3 and DU145 cells (Figures 3 G and H). These data suggested that knockdown of SNHG20 represses PCa cell proliferation and migration.

SNHG20 upregulates the expression of DDX17

Many lncRNAs were reported to function as ceRNAs to relieve the repressive effects of common miRNAs on their genuine targets [30, 35, 36]. Therefore, we investigated the potential targets which are regulated by DDX17 via the ceRNA mechanism. The potential targets were predicted by starBase (<http://starbase.sysu.edu.cn/>) and shown in Table II [43]. DDX17 was the top hit, which has 26 shared miRNAs with SNHG20. Furthermore, DDX17 was reported to have oncogenic roles in breast cancer, colon cancer, and non-small cell lung cancer [44–46]. Thus, we further investigated the effects of SNHG20 on DDX17. miRNAs are known to bind the 3'UTR of target genes and repress 3'UTR activity [47–49]. Thus, we first investigated the effects of SNHG20 on DDX17 3'UTR activity. The 3'UTR of DDX17 was cloned into the luciferase reporter pmirGLO. Dual luciferase reporter assays indicated that enhanced expression of SNHG20 significantly increased the luciferase activity of the constructed reporter containing 3'UTR of DDX17 (Figure 4 A). Conversely, knockdown of SNHG20 significantly decreased the luciferase activity of the constructed reporter containing 3'UTR of DDX17 (Figure 4 B). The mRNA and protein expression levels of DDX17 in SNHG20 stably over-

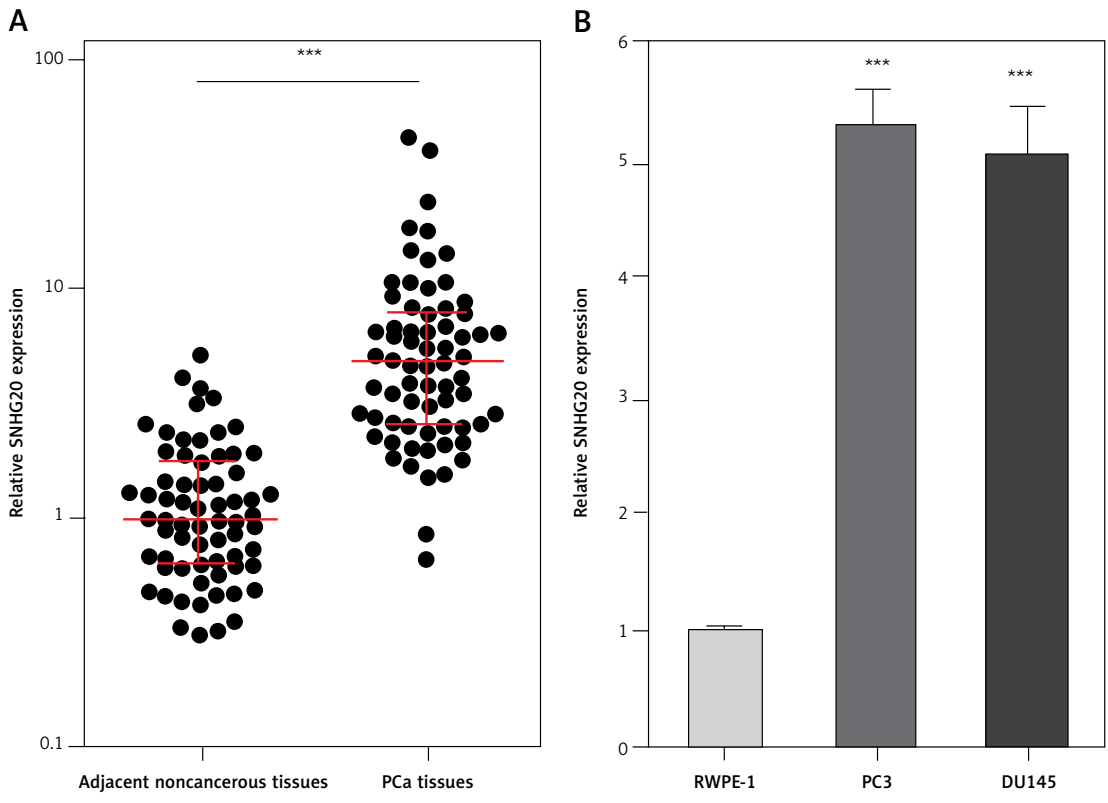


Figure 1. SNHG20 is increased in PCa tissues and cell line. **A** – The expression level of SNHG20 in 68 pairs of PCa tissues and adjacent noncancerous tissues was analyzed by RT-qPCR. Results are displayed as median with inter-quartile range. *** $p < 0.0001$ by Wilcoxon signed-rank test. **B** – The expression level of SNHG20 in human prostate epithelial cell line RWPE-1 and PCa cell lines PC3 and DU145 was analyzed by RT-qPCR. Results are presented as mean \pm SD. *** $p < 0.001$ compared with RWPE-1 group by one-way ANOVA followed by Dunnett’s multiple comparison tests

Table I. The relationship between SNHG20 expression level and clinicopathological characteristics in our PCa cases.

Parameters	N (case)	SNHG20		P-value
		Low	High	
Age [years]:				0.318
< 65	26	15	11	
≥ 65	42	19	23	
PSA level [ng/ml]:				0.144
< 10	15	10	5	
≥ 10	53	24	29	
Gleason score:				0.015
≤ 7	38	24	14	
> 7	30	10	20	
Tumor stage:				0.008
$\leq T2b$	33	22	11	
$\geq T2c$	35	12	23	
Lymph node metastasis:				0.056
N0	56	31	25	
N1	12	3	9	

P-value was acquired by Pearson χ^2 test.

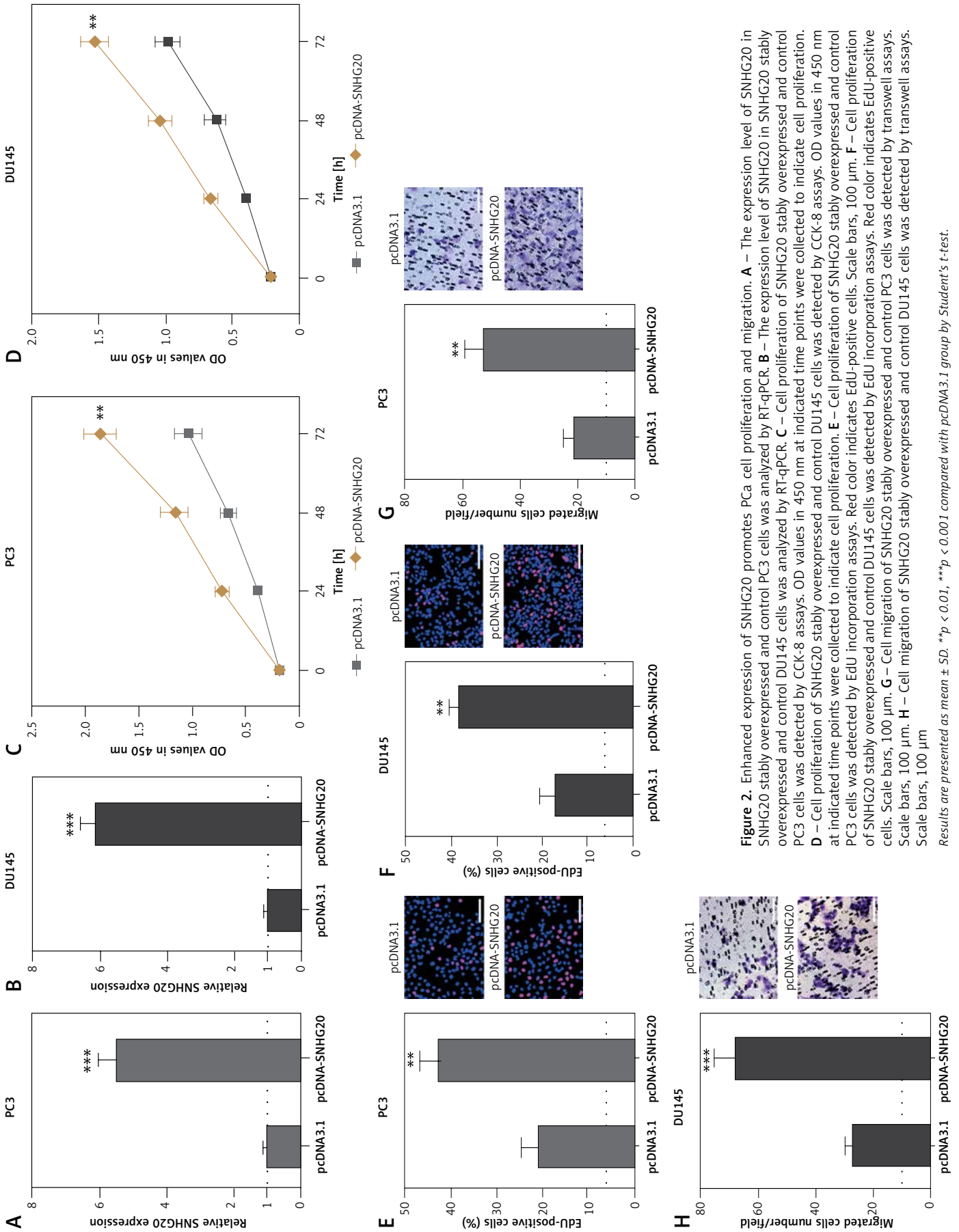


Figure 2. Enhanced expression of SNHG20 promotes Pca cell proliferation and migration. **A** – The expression level of SNHG20 in SNHG20 stably overexpressed and control PC3 cells was analyzed by RT-qPCR. **B** – The expression level of SNHG20 in SNHG20 stably overexpressed and control DU145 cells was analyzed by RT-qPCR. **C** – Cell proliferation of SNHG20 stably overexpressed and control PC3 cells was detected by CCK-8 assays. OD values in 450 nm at indicated time points were collected to indicate cell proliferation. **D** – Cell proliferation of SNHG20 stably overexpressed and control DU145 cells was detected by CCK-8 assays. OD values in 450 nm at indicated time points were collected to indicate cell proliferation. **E** – Cell proliferation of SNHG20 stably overexpressed and control PC3 cells was detected by Edu incorporation assays. Red color indicates Edu-positive cells. Scale bars, 100 μ m. **F** – Cell proliferation of SNHG20 stably overexpressed and control DU145 cells was detected by Edu incorporation assays. Red color indicates Edu-positive cells. Scale bars, 100 μ m. **G** – Cell migration of SNHG20 stably overexpressed and control PC3 cells was detected by transwell assays. Scale bars, 100 μ m. **H** – Cell migration of SNHG20 stably overexpressed and control DU145 cells was detected by transwell assays. Scale bars, 100 μ m

Results are presented as mean \pm SD. ***p* < 0.01, ****p* < 0.001 compared with pcDNA3.1 group by Student's t-test.

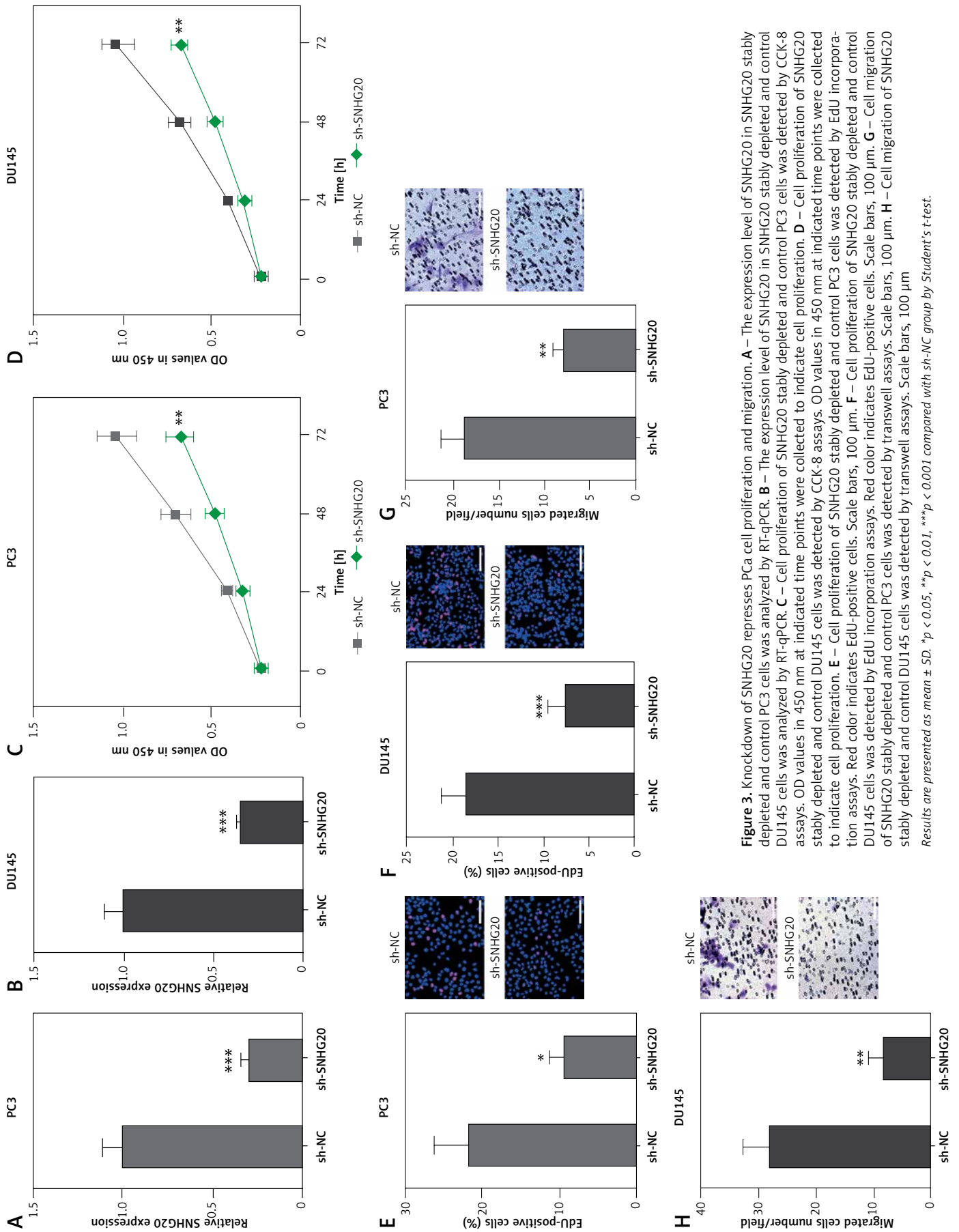


Figure 3. Knockdown of SNHG20 represses PCa cell proliferation and migration. **A** – The expression level of SNHG20 in SNHG20 stably depleted and control PC3 cells was analyzed by RT-qPCR. **B** – The expression level of SNHG20 in SNHG20 stably depleted and control DU145 cells was analyzed by RT-qPCR. **C** – Cell proliferation of SNHG20 stably depleted and control PC3 cells was detected by CCK-8 assays. OD values in 450 nm at indicated time points were collected to indicate cell proliferation. **D** – Cell proliferation of SNHG20 stably depleted and control DU145 cells was detected by CCK-8 assays. OD values in 450 nm at indicated time points were collected to indicate cell proliferation. **E** – Cell proliferation of SNHG20 stably depleted and control PC3 cells was detected by EdU incorporation assays. Red color indicates EdU-positive cells. Scale bars, 100 μ m. **F** – Cell proliferation of SNHG20 stably depleted and control DU145 cells was detected by EdU incorporation assays. Red color indicates EdU-positive cells. Scale bars, 100 μ m. **G** – Cell migration of SNHG20 stably depleted and control PC3 cells was detected by transwell assays. Scale bars, 100 μ m. **H** – Cell migration of SNHG20 stably depleted and control DU145 cells was detected by transwell assays. Scale bars, 100 μ m. Results are presented as mean \pm SD. * p < 0.05, ** p < 0.01, *** p < 0.001 compared with sh-NC group by Student's t-test.

Table II. The predicted ceRNAs of SNHG20

ceRNA name	Gene ID	Gene name	Gene type	Hit MiR num	P-value	FDR
SNHG20	ENSG00000100201	DDX17	Protein_coding	26	2.80E-04	4.63E-04
SNHG20	ENSG00000011021	CLCN6	Protein_coding	25	1.60E-03	1.60E-03
SNHG20	ENSG00000128487	SPECC1	Protein_coding	24	1.05E-04	2.64E-04
SNHG20	ENSG00000080815	PSEN1	Protein_coding	22	9.10E-04	1.05E-03
SNHG20	ENSG00000155858	LSM11	Protein_coding	21	2.78E-04	4.63E-04
SNHG20	ENSG00000120071	KANSL1	Protein_coding	20	1.21E-03	1.30E-03
SNHG20	ENSG00000158805	ZNF276	Protein_coding	19	5.69E-05	2.64E-04
SNHG20	ENSG00000116852	KIF21B	Protein_coding	19	6.18E-04	7.73E-04
SNHG20	ENSG00000157851	DPYSL5	Protein_coding	16	5.43E-04	7.40E-04
SNHG20	ENSG00000213352	GAPDHP44	Processed_pseudogene	13	1.29E-06	1.93E-05
SNHG20	ENSG00000101298	SNPH	Protein_coding	13	6.20E-05	2.64E-04
SNHG20	ENSG00000126368	NR1D1	Protein_coding	10	5.28E-05	2.64E-04
SNHG20	ENSG00000230593	PPIAP40	Processed_pseudogene	8	1.02E-04	2.64E-04
SNHG20	ENSG00000213226	AC242426.1	Processed_pseudogene	7	3.19E-05	2.39E-04
SNHG20	ENSG00000203650	LINC01285	LincRNA	5	1.39E-04	2.64E-04

expressed and depleted PC3 cells were detected by RT-qPCR and western blot, respectively. As displayed in Figures 4 C and D, enhanced expression of SNHG20 upregulated DDX17 mRNA level, while knockdown of SNHG20 downregulated DDX17 mRNA level. Furthermore, enhanced expression of SNHG20 also increased DDX17 protein level, while knockdown of SNHG20 decreased DDX17 protein level (Figures 4 E and F). Taken together, these data suggested that SNHG20 upregulates the expression of DDX17 via the ceRNA mechanism.

Expression level of DDX17 is positively associated with that of SNHG20 in human PCa tissues

Next, the mRNA and protein levels of SNHG20 in PCa cell lines PC3 and DU145 and the human prostate epithelial cell line RWPE-1 were measured by RT-qPCR and western blot. As shown in Figures 5 A and B, consistent with SNHG20, DDX17 mRNA and protein levels were also markedly increased in PCa cell lines compared with the prostate epithelial cell line. In order to verify whether the positive regulation of DDX17 by SNHG20 exists *in vivo*, the mRNA level of DDX17 in the same 68 pairs of PCa tissues and adjacent noncancerous tissues used in Figure 1 was detected by RT-qPCR. As shown in Figure 5 C, DDX17 was also significantly increased in PCa tissues compared with adjacent noncancerous tissues. We further analyzed the correlation

between the expression level of DDX17 and that of SNHG20 in these 68 PCa tissues. As shown in Figure 5 D, the RNA level of DDX17 was significantly positively associated with that of SNHG20 in PCa tissues ($r = 0.7331$, $p < 0.0001$).

DDX17 promotes PCa cell proliferation and migration

Although DDX17 has been reported to have oncogenic roles in breast cancer, colon cancer, and non-small cell lung cancer, the biological roles of DDX17 in PCa are still unclear. Thus, we further investigated the roles of DDX17 in PCa cell proliferation and migration. DDX17 stably overexpressed and control PC3 cells were constructed through the stable transfection of DDX17 overexpression vector or control empty vector. The enhanced expression of DDX17 was verified by western blot (Figure 6 A). CCK-8 assays indicated that enhanced expression of DDX17 markedly promoted cell proliferation of PC3 cells (Figure 6 B). EdU incorporation assays further verified that enhanced expression of DDX17 markedly promoted cell proliferation of PC3 cells (Figure 6 C). Subsequently, we investigated the roles of DDX17 in PCa cell migration. Transwell assays revealed that enhanced expression of DDX17 significantly promoted cell migration of PC3 cells (Figure 6 D). These results demonstrated that DDX17 also has oncogenic roles in PCa.

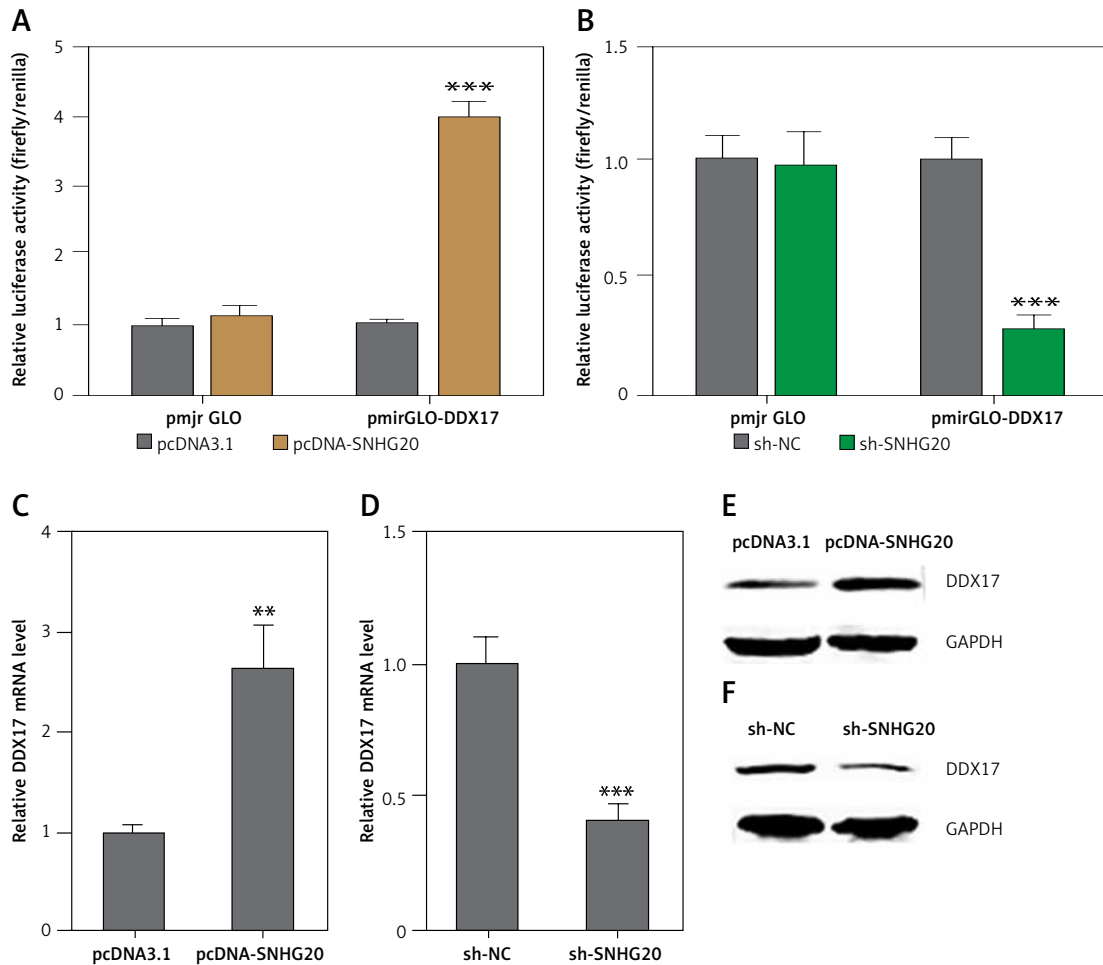


Figure 4. SNHG20 upregulates the expression of DDX17. **A** – Luciferase activity in PC3 cells co-transfected with luciferase reporters containing DDX17 3’UTR or nothing and SNHG20 overexpression vector (pcDNA-SNHG20) or control empty vector (pcDNA3.1). Results are displayed as the relative ratio of firefly luciferase activity to Renilla luciferase activity. **B** – Luciferase activity in PC3 cells co-transfected with luciferase reporters containing DDX17 3’UTR or nothing and SNHG20 knockdown vector (sh-SNHG20) or negative control vector (sh-NC). Results are displayed as the relative ratio of firefly luciferase activity to Renilla luciferase activity. **C** – The mRNA level of DDX17 in SNHG20 stably overexpressed and control PC3 cells was analyzed by RT-qPCR. **D** – The mRNA level of DDX17 in SNHG20 stably depleted and control PC3 cells was analyzed by RT-qPCR. **E** – The protein level of DDX17 in SNHG20 stably overexpressed and control PC3 cells was analyzed by western blot. **F** – The protein level of DDX17 in SNHG20 stably depleted and control PC3 cells was analyzed by western blot

Results are presented as mean ± SD. ***p* < 0.01, ****p* < 0.001 compared with pcDNA3.1 or sh-NC group by Student’s *t*-test.

Depletion of DDX17 reverses the roles of SNHG20 in promoting PCa cell proliferation and migration

To verify whether SNHG20 promotes PCa cell proliferation and migration via the upregulation of DDX17, we stably depleted DDX17 in SNHG20 stably overexpressed PC-3 cells via the stable transfection of DDX17 knockdown vector (sh-DDX17). The knockdown of DDX17 was verified by western blot (Figure 7 A). CCK-8 assays indicated that knockdown of DDX17 attenuated the pro-proliferative roles of SNHG20 overexpression (Figures 7 B). EdU incorporation assays further verified that knockdown of DDX17 reversed the pro-proliferative roles of SNHG20

overexpression (Figure 7 C). Transwell assays revealed that knockdown of DDX17 attenuated the pro-migratory roles of SNHG20 overexpression (Figure 7 D). These results demonstrated that knockdown of DDX17 reverses the roles of SNHG20 in promoting PCa cell proliferation and migration.

Discussion

As a class of novel regulatory RNAs, lncRNAs are revealed to have various roles in PCa [50–54]. lncRNA TMPO-AS1 is reported to promote PCa cell proliferation and migration [50]. DDX5/p68 associated lncRNA LOC284454 is reduced in PCa [51]. lncRNA LINC00844 prevents PCa cell migration

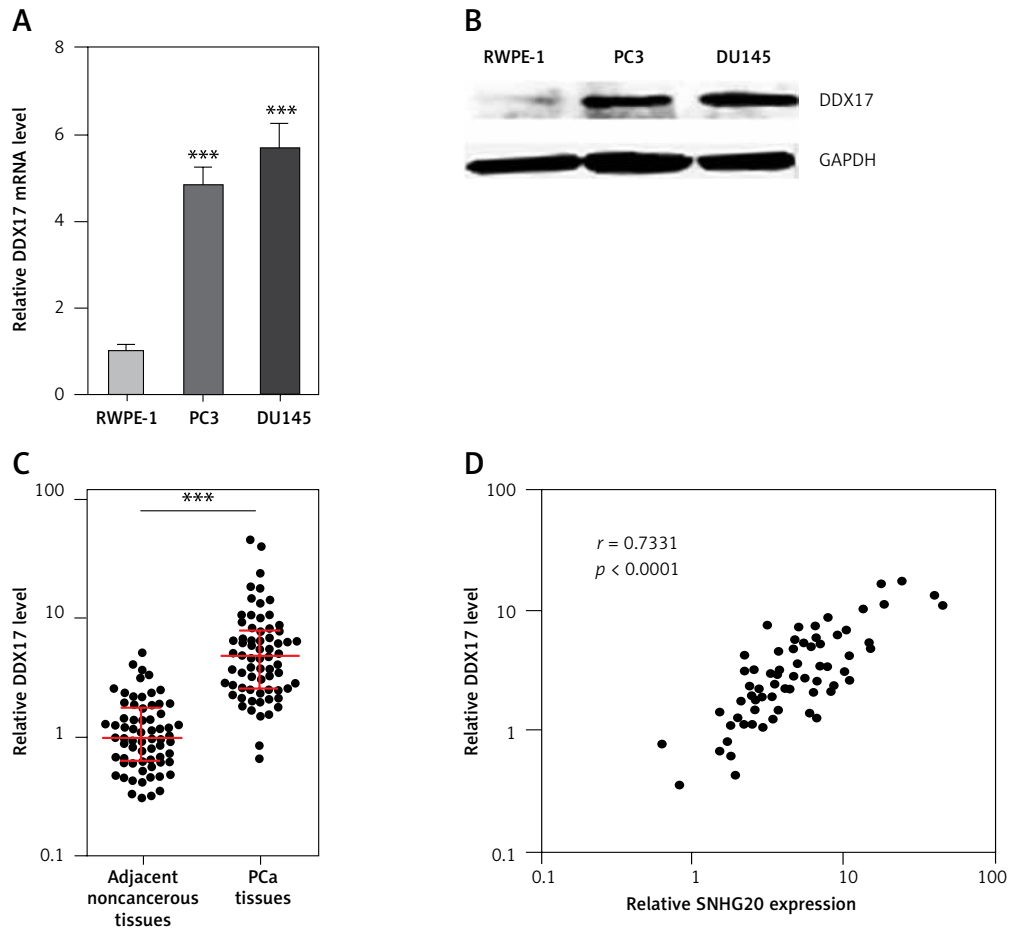


Figure 5. The relationship between SNHG20 and DDX17 expression levels in PCa tissues. **A** – DDX17 mRNA level in human prostate epithelial cell line RWPE-1 and PCa cell lines PC3 and DU145 was analyzed by RT-qPCR. Results are presented as mean \pm SD. $***p < 0.001$ compared with RWPE-1 group by one-way ANOVA followed by Dunnett’s multiple comparison tests. **B** – DDX17 protein level in human prostate epithelial cell line RWPE-1 and PCa cell lines PC3 and DU145 was analyzed by western blot. **C** – DDX17 mRNA level in 68 pairs of PCa tissues and adjacent noncancerous tissues was analyzed by RT-qPCR. Results are displayed as median with interquartile range. $***p < 0.0001$ by Wilcoxon signed-rank test. **D** – The correlation between DDX17 and SNHG20 expression level in PCa tissues was analyzed by Pearson correlation analysis. $n = 68$, $r = 0.7331$, $p < 0.0001$

and invasion via facilitating androgen receptor binding to the chromatin [52]. LncRNA MIR222HG facilitates PCa development via affecting miRNAs-mediated expression silencing [53]. LncRNA SchLAP1 promotes aggressive PCa via antagonizing the SWI/SNF complex [54]. Due to the huge number of lncRNAs in humans, other lncRNAs may also play important roles in PCa. In the present study, we identified lncRNA SNHG20 as a novel oncogene in PCa. Our data revealed that SNHG20 is highly expressed in PCa tissues and cell lines compared with adjacent noncancerous tissues and the prostate epithelial cell line, respectively. Moreover, we revealed that high expression of SNHG20 is positively associated with high Gleason score and advanced tumor stages. Gain-of-function and loss-of-function experiments revealed that enhanced expression of SNHG20 promotes PCa cell proliferation and migration, while knock-down of SNHG20 represses PCa cell proliferation

and migration. Therefore, our data suggested that SNHG20 acts as an oncogene in PCa.

Several lncRNAs have been verified to function as ceRNAs via competitively binding common miRNAs [35, 36, 41]. Thus, we further explored the potential of SNHG20 acting as a ceRNA in PCa. Using starBase, we objectively screened all the targets which share common miRNAs with SNHG20. DDX17 was identified to share 26 common miRNAs with SNHG20. In clinical samples, we further found that consistent with SNHG20, DDX17 was also highly expressed in PCa tissues. In addition, the expression of DDX17 was significantly positively associated with that of SNHG20 in PCa tissues, which further supports the potential regulation of DDX17 by SNHG20. Indeed, dual luciferase reporter assays, RT-qPCR, and western blot experiments all verified that SNHG20 increased 3’UTR activity, mRNA level, and protein level of DDX17 in PCa cells, which

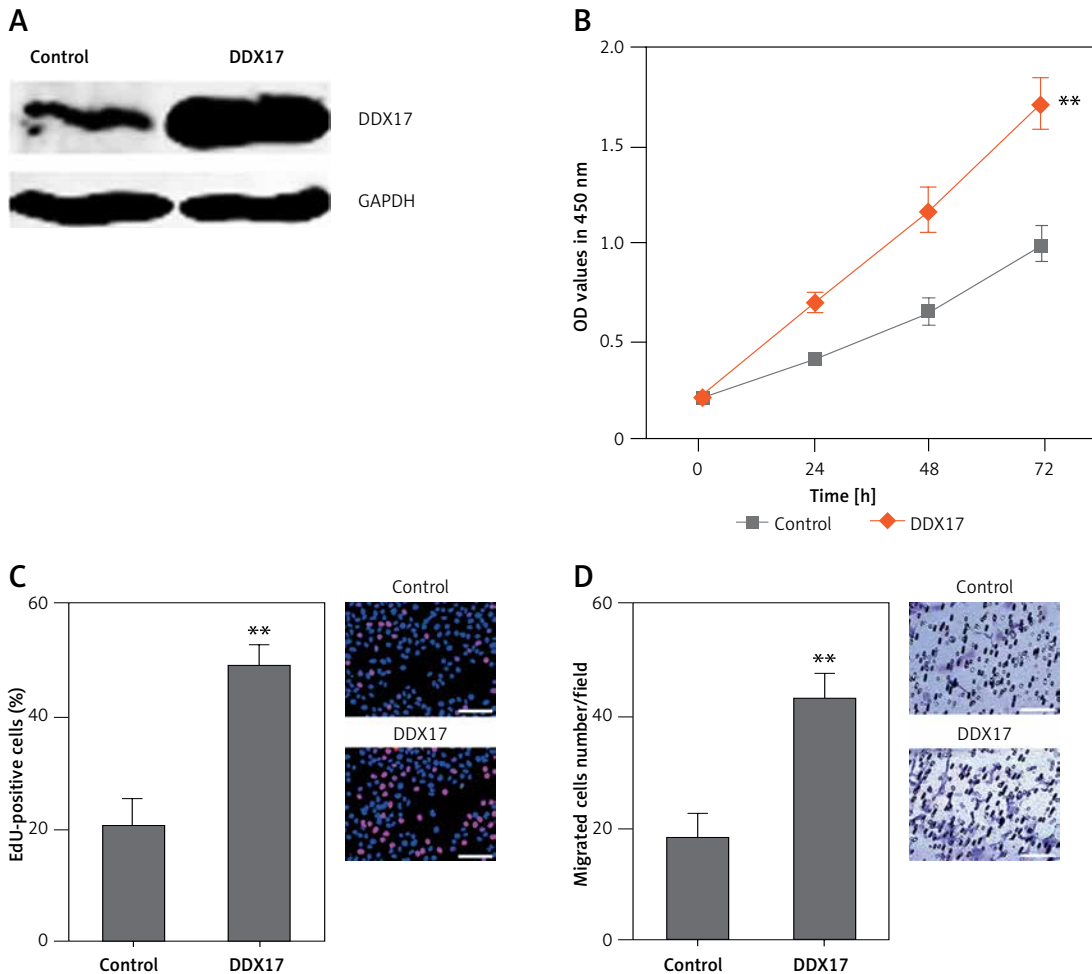


Figure 6. DDX17 promotes PCa cell proliferation and migration. **A** – The expression level of DDX17 in DDX17 stably overexpressed and control PC3 cells was analyzed by western blot. **B** – Cell proliferation of DDX17 stably overexpressed and control PC3 cells was detected by CCK-8 assays. OD values at 450 nm at indicated time points were collected to indicate cell proliferation. **C** – Cell proliferation of DDX17 stably overexpressed and control PC3 cells was detected by EdU incorporation assays. Red color indicates EdU-positive cells. Scale bars, 100 μ m. **D** – Cell migration of DDX17 stably overexpressed and control PC3 cells was detected by transwell assays. Scale bars, 100 μ m. Results are presented as mean \pm SD. ** $p < 0.01$ compared with control group by Student's *t*-test.

support that SNHG20 upregulates DDX17 expression via a ceRNA mechanism.

DDX17 is a DEAD box RNA helicase. DDX17 has been shown to have oncogenic roles in colon cancer, breast cancer, and non-small cell lung cancer [44–46]. Furthermore, one of the reported functions of DDX17 is to act as a transcriptional co-regulator of various transcription factors, including estrogen receptor and androgen receptor [55]. Therefore, we further investigated the biological roles of DDX17 in PCa. Gain-of-function experiments revealed that, consistent with SNHG20, enhanced expression of DDX17 also significantly promotes PCa cell proliferation and migration. Moreover, depletion of DDX17 reverses the roles of SNHG20 in promoting PCa cell proliferation and migration. These data suggest that the upregulation of DDX17 at least partially mediates the oncogenic roles of SNHG20 in PCa. Further ex-

ploration of the downstream targets of SNHG20/DDX17 would promote better understanding of the mechanisms of action of SNHG20.

In conclusion, collectively, our results show that lncRNA SNHG20 is highly expressed in PCa and associated with advanced tumor stages. SNHG20 promotes PCa cell proliferation and migration via acting as a ceRNA and further upregulating DDX17. Our data imply that SNHG20 may be a novel potential therapeutic target for PCa.

Conflict of interest

The authors declare no conflict of interest.

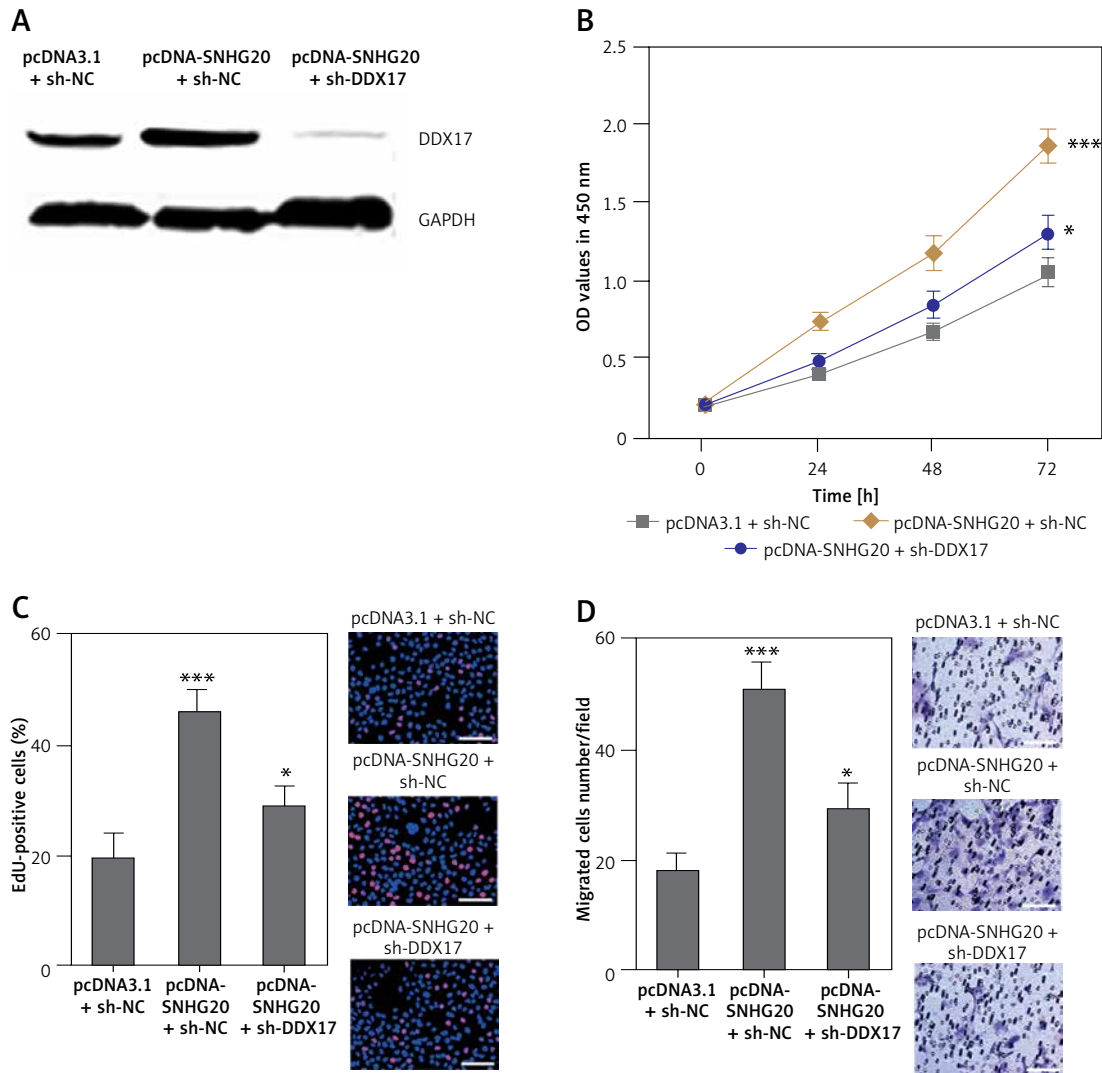


Figure 7. Depletion of DDX17 reverses the roles of SNHG20 in promoting PCa cell proliferation and migration. **A** – The expression level of DDX17 in SNHG20 stably overexpressed and concurrently DDX17 stably depleted PC3 cells was analyzed by western blot. **B** – Cell proliferation of SNHG20 stably overexpressed and concurrently DDX17 stably depleted PC3 cells was detected by CCK-8 assays. OD values in 450 nm at indicated time points were collected to indicate cell proliferation. **C** – Cell proliferation of SNHG20 stably overexpressed and concurrently DDX17 stably depleted PC3 cells was detected by EdU incorporation assays. Red color indicates EdU-positive cells. Scale bars, 100 μ m. **D** – Cell migration of SNHG20 stably overexpressed and concurrently DDX17 stably depleted PC3 cells was detected by transwell assays. Scale bars, 100 μ m

Results are presented as mean \pm SD. * $p < 0.05$, *** $p < 0.001$ compared with pcDNA3.1 + sh-NC group by one-way ANOVA followed by Dunnett's multiple comparison tests.

References

- Bray F, Ferlay J, Soerjomataram I, Siegel RL, Torre LA, Jemal A. Global cancer statistics 2018: GLOBOCAN estimates of incidence and mortality worldwide for 36 cancers in 185 countries. *CA Cancer J Clin* 2018; 68: 394-424.
- Cuzick J, Thorat MA, Andriole G, et al. Prevention and early detection of prostate cancer. *Lancet Oncol* 2014; 15: e484-92.
- Lane JA, Donovan JL, Davis M, et al. Active monitoring, radical prostatectomy, or radiotherapy for localised prostate cancer: study design and diagnostic and baseline results of the ProtecT randomised phase 3 trial. *Lancet Oncol* 2014; 15: 1109-18.
- Teply BA, Wang H, Lubber B, et al. Bipolar androgen therapy in men with metastatic castration-resistant prostate cancer after progression on enzalutamide: an open-label, phase 2, multicohort study. *Lancet Oncol* 2018; 19: 76-86.
- Bluemn EG, Coleman IM, Lucas JM, et al. Androgen receptor pathway-independent prostate cancer is sustained through FGF signaling. *Cancer Cell* 2017; 32: 474-89e6.
- Piastowska-Ciesielska AW, Kozłowski M, Wagner W, Dominska K, Ochedalski T. Effect of an angiotensin II type 1 receptor blocker on caveolin-1 expression in prostate cancer cells. *Arch Med Sci* 2013; 9: 739-44.
- Iyer MK, Niknafs YS, Malik R, et al. The landscape of long noncoding RNAs in the human transcriptome. *Nat Genet* 2015; 47: 199-208.

8. Ponting CP, Oliver PL, Reik W. Evolution and functions of long noncoding RNAs. *Cell* 2009; 136: 629-41.
9. Fatica A, Bozzoni I. Long non-coding RNAs: new players in cell differentiation and development. *Nat Rev Genet* 2014; 15: 7-21.
10. Wang Z, Yang B, Zhang M, et al. lncRNA epigenetic landscape analysis identifies EPIC1 as an oncogenic lncRNA that interacts with MYC and promotes cell-cycle progression in cancer. *Cancer Cell* 2018; 33: 706-20e9.
11. Hu WL, Jin L, Xu A, et al. GUARDIN is a p53-responsive long non-coding RNA that is essential for genomic stability. *Nat Cell Biol* 2018; 20: 492-502.
12. Berger AC, Korkut A, Kanchi RS, et al. A comprehensive pan-cancer molecular study of gynecologic and breast cancers. *Cancer Cell* 2018; 33: 690-705e9.
13. Zhang C, Yuan J, Hu H, et al. Long non-coding RNA CH-CHD4P4 promotes epithelial-mesenchymal transition and inhibits cell proliferation in calcium oxalate-induced kidney damage. *Braz J Med Biol Res* 2017; 51: e6536.
14. Kang K, Huang YH, Li HP, Guo SM. Expression of UCA1 and MALAT1 long-chain non-coding RNAs in esophageal squamous cell carcinoma tissues is predictive of patient prognosis. *Arch Med Sci* 2018; 14: 752-9.
15. Mondal T, Juvvuna PK, Kirkeby A, et al. Sense-antisense lncRNA pair encoded by locus 6p22.3 determines neuroblastoma susceptibility via the USP36-CHD7-SOX9 regulatory axis. *Cancer Cell* 2018; 33: 417-34e7.
16. Yuan JH, Liu XN, Wang TT, et al. The MBNL3 splicing factor promotes hepatocellular carcinoma by increasing PXN expression through the alternative splicing of lncRNA-PXN-AS1. *Nat Cell Biol* 2017; 19: 820-32.
17. Chen JF, Wu P, Xia R, et al. STAT3-induced lncRNA HAGLROS overexpression contributes to the malignant progression of gastric cancer cells via mTOR signal-mediated inhibition of autophagy. *Mol Cancer* 2018; 17: 6.
18. Zhou K, Zhang C, Yao H, et al. Knockdown of long non-coding RNA NEAT1 inhibits glioma cell migration and invasion via modulation of SOX2 targeted by miR-132. *Mol Cancer* 2018; 17: 105.
19. Zhu XT, Yuan JH, Zhu TT, Li YY, Cheng XY. Long noncoding RNA glypican 3 (GPC3) antisense transcript 1 promotes hepatocellular carcinoma progression via epigenetically activating GPC3. *FEBS J* 2016; 283: 3739-54.
20. Zheng P, Li H, Xu P, et al. High lncRNA HULC expression is associated with poor prognosis and promotes tumor progression by regulating epithelial-mesenchymal transition in prostate cancer. *Arch Med Sci* 2018; 14: 679-86.
21. Luo Z, Pan J, Ding Y, Zhang YS, Zeng Y. The function and clinical relevance of lncRNA UBE2CP3-001 in human gliomas. *Arch Med Sci* 2018; 14: 1308-20.
22. Lin A, Hu Q, Li C, et al. The LINK-A lncRNA interacts with PtdIns(3,4,5)P3 to hyperactivate AKT and confer resistance to AKT inhibitors. *Nat Cell Biol* 2017; 19: 238-51.
23. Grelet S, Link LA, Howley B, et al. A regulated PNUITS mRNA to lncRNA splice switch mediates EMT and tumor progression. *Nat Cell Biol* 2017; 19: 1105-15.
24. Tsai KW, Lo YH, Liu H, et al. Linc00659, a long noncoding RNA, acts as novel oncogene in regulating cancer cell growth in colorectal cancer. *Mol Cancer* 2018; 17: 72.
25. Li JK, Chen C, Liu JY, et al. Long noncoding RNA MRCCAT1 promotes metastasis of clear cell renal cell carcinoma via inhibiting NPR3 and activating p38-MAPK signaling. *Mol Cancer* 2017; 16: 111.
26. Yang M, Zhang L, Wang X, Zhou Y, Wu S. Down-regulation of miR-203a by lncRNA PVT1 in multiple myeloma promotes cell proliferation. *Arch Med Sci* 2018; 14: 1333-9.
27. Michelini F, Pitchiaya S, Vitelli V, et al. Damage-induced lncRNAs control the DNA damage response through interaction with DDRNAs at individual double-strand breaks. *Nat Cell Biol* 2017; 19: 1400-11.
28. Zhang L, Yang F, Yuan JH, et al. Epigenetic activation of the MiR-200 family contributes to H19-mediated metastasis suppression in hepatocellular carcinoma. *Carcinogenesis* 2013; 34: 577-86.
29. Xu D, Yang F, Yuan JH, et al. Long noncoding RNAs associated with liver regeneration 1 accelerates hepatocyte proliferation during liver regeneration by activating Wnt/beta-catenin signaling. *Hepatology* 2013; 58: 739-51.
30. Yuan JH, Yang F, Wang F, et al. A long noncoding RNA activated by TGF-beta promotes the invasion-metastasis cascade in hepatocellular carcinoma. *Cancer Cell* 2014; 25: 666-81.
31. Zhao W, Fu H, Zhang S, Sun S, Liu Y. lncRNA SNHG16 drives proliferation, migration, and invasion of heman-gioma endothelial cell through modulation of miR-520d-3p/STAT3 axis. *Cancer Med* 2018 doi: 10.1002/cam4.1562.
32. Li J, Wu G, Cao Y, Hou Z. Roles of miR-210 in the pathogenesis of pre-eclampsia. *Arch Med Sci* 2019; 15: 183-90.
33. Wang Y, Zeng X, Wang N, et al. Long noncoding RNA DANCR, working as a competitive endogenous RNA, promotes ROCK1-mediated proliferation and metastasis via decoying of miR-335-5p and miR-1972 in osteosarcoma. *Mol Cancer* 2018; 17: 89.
34. Shen Q, Jiang Y. lncRNA NNT-AS1 promotes the proliferation, and invasion of lung cancer cells via regulating miR-129-5p expression. *Biomed Pharmacother* 2018; 105: 176-81.
35. Salmena L, Poliseno L, Tay Y, Kats L, Pandolfi PP. A ceRNA hypothesis: the Rosetta Stone of a hidden RNA language? *Cell* 2011; 146: 353-8.
36. Liang H, Yu T, Han Y, et al. lncRNA PTAR promotes EMT and invasion-metastasis in serous ovarian cancer by competitively binding miR-101-3p to regulate ZEB1 expression. *Mol Cancer* 2018; 17: 119.
37. Li C, Zhou L, He J, Fang XQ, Zhu SW, Xiong MM. Increased long noncoding RNA SNHG20 predicts poor prognosis in colorectal cancer. *BMC Cancer* 2016; 16: 655.
38. Liu J, Lu C, Xiao M, Jiang F, Qu L, Ni R. Long non-coding RNA SNHG20 predicts a poor prognosis for HCC and promotes cell invasion by regulating the epithelial-to-mesenchymal transition. *Biomed Pharmacother* 2017; 89: 857-63.
39. Cui N, Liu J, Xia H, Xu D. lncRNA SNHG20 contributes to cell proliferation and invasion by upregulating ZFX expression sponging miR-495-3p in gastric cancer. *J Cell Biochem* 2019; 120: 3114-23.
40. Zhang J, Ju C, Zhang W, Xie L. lncRNA SNHG20 is associated with clinical progression and enhances cell migration and invasion in osteosarcoma. *IUBMB life* 2018; 70: 1115-21.
41. Guo H, Yang S, Li S, Yan M, Li L, Zhang H. lncRNA SNHG20 promotes cell proliferation and invasion via miR-140-5p-ADAM10 axis in cervical cancer. *Biomed Pharmacother* 2018; 102: 749-57.
42. Chen Z, Chen X, Chen P, et al. Long non-coding RNA SNHG20 promotes non-small cell lung cancer cell proliferation and migration by epigenetically silencing of P21 expression. *Cell Death Dis* 2017; 8: e3092.
43. Li JH, Liu S, Zhou H, Qu LH, Yang JH. starBase v2.0: decoding miRNA-ceRNA, miRNA-ncRNA and protein-RNA interaction networks from large-scale CLIP-Seq data. *Nucleic Acids Res* 2014; 42: D92-7.

44. Alqahtani H, Gopal K, Gupta N, et al. DDX17 (P72), a Sox2 binding partner, promotes stem-like features conferred by Sox2 in a small cell population in estrogen receptor-positive breast cancer. *Cell Signal* 2016; 28: 42-50.
45. Janknecht R. Multi-talented DEAD-box proteins and potential tumor promoters: p68 RNA helicase (DDX5) and its paralog, p72 RNA helicase (DDX17). *Am J Transl Res* 2010; 2: 223-34.
46. Li K, Mo C, Gong D, et al. DDX17 nucleocytoplasmic shuttling promotes acquired gefitinib resistance in non-small cell lung cancer cells via activation of beta-catenin. *Cancer Lett* 2017; 400: 194-202.
47. Yuan JH, Yang F, Chen BF, et al. The histone deacetylase 4/SP1/microrna-200a regulatory network contributes to aberrant histone acetylation in hepatocellular carcinoma. *Hepatology* 2011; 54: 2025-35.
48. Wu MZ, Cheng WC, Chen SF, et al. miR-25/93 mediates hypoxia-induced immunosuppression by repressing cGAS. *Nat Cell Biol* 2017; 19: 1286-96.
49. Bu Y, Yoshida A, Chitnis N, et al. A PERK-miR-211 axis suppresses circadian regulators and protein synthesis to promote cancer cell survival. *Nat Cell Biol* 2018; 20: 104-15.
50. Huang W, Su X, Yan W, et al. Overexpression of AR-regulated lncRNA TMPO-AS1 correlates with tumor progression and poor prognosis in prostate cancer. *Prostate* 2018; 78: 1248-61.
51. Das M, Renganathan A, Dighe SN, et al. DDX5/p68 associated lncRNA LOC284454 is differentially expressed in human cancers and modulates gene expression. *RNA Biol* 2018; 15: 214-30.
52. Lingadahalli S, Jadhao S, Sung YY, et al. Novel lncRNA LINC00844 regulates prostate cancer cell migration and invasion through AR Signaling. *Mol Cancer Res* 2018; 16: 1865-78.
53. Sun T, Du SY, Armenia J, et al. Expression of lncRNA MIR222HG co-transcribed from the miR-221/222 gene promoter facilitates the development of castration-resistant prostate cancer. *Oncogenesis* 2018; 7: 30.
54. Prensner JR, Iyer MK, Sahu A, et al. The long noncoding RNA SchLAP1 promotes aggressive prostate cancer and antagonizes the SWI/SNF complex. *Nat Genet* 2013; 45: 1392-8.
55. Samaan S, Tranchevent LC, Dardenne E, et al. The Ddx5 and Ddx17 RNA helicases are cornerstones in the complex regulatory array of steroid hormone-signaling pathways. *Nucleic Acids Res* 2014; 42: 2197-207.